James, F., & Roos, M. (1975) *Comput. Phys. Commun. 10*, 343-367.
Junesch, U., & Graberr, P. (1987) *Biochim. Biophys. Acta 893*, 275-288.
Leckband, D., & Hammes, G. G. (1987) *Biochemistry 26*, 2306-2312.
McCarty, R. E., & Carmeli, C. (1982) in *Photosynthesis: Energy conversion by Plants and Bacteria* (Govindjee, Ed.) Vol. 1, pp 647-695, Academic Press, New York.
Monod, J., Wyman, J., & Changeux, J. P. (1965) *J. Mol. Biol. 12*, 88-118.
Morony, J. V., Lopreti, L., McEwen, B. F., McCarty, R. E., & Hammes, G. G. (1983) *FEBS Lett. 158*, 58-62.
Nelder, J. A., & Mead, R. (1965) *Comput. J. 7*, 308-312.
Rosen, G., Gresser, M., Vinkler, C., & Boyer, P. D. (1979) *J. Biol. Chem. 254*, 10654-10661.
Ryan, J., & Ryan, D. (1976) *MINITAB Student Handbook*, Duxbury Press, New York.
Segel, L. A. (1980) *Mathematical Models in Molecular and Cellular Biology*, pp 39-55, Cambridge University Press, Cambridge.
Stroop, S. D., Boyer, P. D. (1987) *Biochemistry 26*, 1479-1484.
Strotmann, H., & Bickel-Sandkotter, S. (1977) *Biochim. Biophys. Acta 400*, 126-135.
Takabe, T., Debenedetti, E., & Jagendorf, A. T. (1982) *Biochim. Biophys. Acta 682*, 11-20.
Wu, D., & Boyer, P. D. (1986) *Biochemistry 25*, 3390-3396.
Zhixiong, X., Jun-Mei, Z., Melese, T., Cross, R., & Boyer, P. D. (1987) *Biochemistry 26*, 3749-3753.

^1H and ^{31}P Nuclear Magnetic Resonance and Kinetic Studies of the Active Site Structure of Chloroplast CF_1 ATP Synthase†

Cathy C. Devlin and Charles M. Grisham*
Department of Chemistry, University of Virginia, Charlottesville, Virginia 22901
Received September 13, 1989; Revised Manuscript Received February 5, 1990

ABSTRACT: The interaction of nucleotides and nucleotide analogues and their metal complexes with Mn^{2+} bound to both the latent and dithiothreitol-activated CF_1 ATP synthase has been examined by means of steady-state kinetics, water proton relaxation rate (PRR) measurements, and ^1H and ^{31}P nuclear relaxation measurements. Titration of both the latent and activated Mn^{2+}-CF_1 complexes with ATP, ADP, P_i, $Co(NH_3)_4ATP$, $Co(NH_3)_4ADP$, and $Co(NH_3)_4AMPPCP$ leads to increases in the water relaxation enhancement, consistent with enhanced metal binding and a high ternary complex enhancement. Steady-state kinetic studies are consistent with competitive inhibition of CF_1 by $Co(NH_3)_4AMPPCP$ with respect to CaATP. The data are consistent with a K_i for $Co(NH_3)_4AMPPCP$ of 650 μM, in good agreement with a previous K_i of 724 μM for $Cr(H_2O)_4ATP$ [Frasch, W., & Selman, B. (1982) *Biochemistry 21*, 3636-3643], and a best fit K_D of 209 μM from the water PRR measurements. ^1H and ^{31}P nuclear relaxation measurements in solutions of CF_1 and $Co(NH_3)_4AMPPCP$ were used to determine the conformation of the bound substrate analogue and the arrangement with respect to this structure of high- and low-affinity sites for Mn^{2+}. The bound nucleotide analogue adopts a bent conformation, with the low-affinity Mn^{2+} site situated between the adenine and triphosphate moieties and the high-affinity metal site located on the far side of the triphosphate chain. The low-affinity metal forms a distorted inner-sphere complex with the β-P and γ-P of the substrate. The distances from Mn^{2+} to the triphosphate chain are too large for first coordination sphere complexes but are appropriate for second-sphere complexes involving, for example, intervening hydrogen-bonded water molecules or residues from the protein.

Chloroplast coupling factor 1, or CF_1 ATPase,[1] is a latent, soluble membrane protein that couples the synthesis of ATP to proton transport across the thylakoid membranes of green plants. The enzyme has a molecular weight of approximately 400 000, and it exists as an aggregate of five distinct subunits with a stoichiometry of $\alpha_3\beta_3\gamma\delta\epsilon$. Nucleotide binding to the ATPase has been extensively studied by Hammes et al. (Carlier & Hammes, 1979; Bruist & Hammes, 1981; Leckband & Hammes, 1987) while metal binding to the enzyme has been characterized by a number of other researchers (Hochman & Carmeli, 1981; Hiller & Carmeli, 1985; Haddy et al., 1985). The preponderance of the data in these works is consistent with the existence of three nucleotide sites, one of which is believed to be a regulatory ADP binding site, the second of which is believed to bind MgATP with a dissociation half-time on the order of days, and the third of which is believed to be the catalytic site for ADP/ATP turnover. The metal binding studies are consistent with one to three tight,

†Supported by grants from the National Institutes of Health (AM19419), the Muscular Dystrophy Association of America, and the National Science Foundation. The NMR instrumentation used in these studies was provided by grants from the National Science Foundation and the University of Virginia.
* To whom correspondence should be addressed.

[1] Abbreviations: CF_1, chloroplast coupling factor 1; Tricine, *N*-[tris(hydroxymethyl)methyl]glycine; DTT, 1,4-dithio-L-threitol; AMPPCP, adenosine 5'-(β,γ-methylenetriphosphate); CoADP, β,γ-bidentate $Co(NH_3)_4ADP$; CoATP, β,γ-bidentate $Co(NH_3)_4ATP$; Tris, tris(hydroxymethyl)aminomethane; CoAMPPCP, β,γ-bidentate $Co(NH_3)_4AMPPCP$; NMR, nuclear magnetic resonance; EPR, electron paramagnetic resonance; H_{pcp}, protons of the CH_2 group bridging the β- and γ-P of CoAMPPCP.

0006-2960/90/0429-6192$02.50/0

interacting divalent metal binding sites in the absence of added ATP and an additional class of weaker, noninteracting metal sites in the presence of added ATP. The mechanistic characteristics of this enzyme are unusual and not yet fully understood. The approach of our laboratory has been (a) to increase our understanding of metal and nucleotide binding to the CF_1 ATPase in order to better characterize the enzyme mechanism and (b) to attempt to determine the active site structure of this enzyme in order to evaluate possible energy-coupling mechanisms within the context of an established structure.

Nuclear magnetic resonance spectroscopy provides some of the most quantitative and powerful methods for such studies. We have applied a number of these techniques to study metal and nucleotide binding to CF_1 ATPase and to study the active site structure of the enzyme. Two potential problems arise in structural studies involving metals and nucleotides, because the triphosphate moiety of the nucleotide contributes another high-affinity metal binding site to the ATP–ATPase complex and because nucleotide probes are usually susceptible to hydrolysis. Our approach to these problems is the use of a nonhydrolyzable, substitution-inert nucleotide analogue, Co$(NH_3)_4$AMPPCP, in which Co(III) is tightly coordinated to the β- and γ-P of the triphosphate chain. There is a growing body of evidence supporting the relevance of Co(III)- and Cr(III)-nucleotide complexes and their usefulness as structural probes. Previous studies within our laboratory have shown the stability of these complexes in the presence and absence of a variety of ATPases (McClaugherty & Grisham, 1982; Klemens, 1987; Stewart & Grisham, 1988).

In the present work, proton relaxation rate enhancement (PRR) measurements were used to determine binding constants of a variety of nucleotide analogues and substrates to both latent and DTT-activated CF_1 ATPase–Mn^{2+} complex. ^{31}P and ^1H nuclear relaxation measurements of Co$(NH_3)_4$AMPPCP were made in the presence of Mn^{2+} and DTT-activated CF_1 ATPase. The distances from enzyme-bound Mn^{2+} to Co$(NH_3)_4$AMPPCP at the catalytic site are used to map the active site metal binding sites and to determine the conformation of enzyme-bound nucleotide. A preliminary account of the water proton relaxation and ^{31}P relaxation has appeared (Devlin & Grisham, 1988). While the manuscript was being prepared for publication, two papers (Haddy & Sharp, 1989; Haddy et al., 1989) describing water proton and deuteron relaxation studies of Mn^{2+} complexes of latent CF_1 appeared. These papers amplify and corroborate certain aspects of our work, as will be described under Discussion.

Experimental Procedures

Materials. (Diethylaminoethyl)cellulose (DE-23) was purchased from Whatman. ADP, ATP, and AMPPCP were from Sigma Chemical Co. [γ-^{32}P]ATP was from New England Nuclear. The β,γ-bidentate complexes of Co$(NH_3)_4$ATP and Co$(NH_3)_4$ADP were prepared as described by Cornelius et al. (1977). Co$(NH_3)_4$AMPPCP was synthesized by following the procedure for Co$(NH_3)_4$ATP and heating the sample for 14 min rather than the published 10-min value. Vanadate solutions were prepared as outlined by Goodno (1982). Centricon-30 microconcentrators were from Amicon. Deuterium oxide (99.8 atom %) was from Aldrich Chemical Co.; Tris-d_{11} and deuterium oxide (99.98 atom %) were from MSD Isotopes; manganese chloride was from Baker Chemicals. All other reagents were of the highest purity commercially available.

Enzyme Preparation. CF_1 ATPase was isolated from fresh market spinach according to the method of Binder et al. (1978) with modifications as described by Cerione et al. (1983). The crude ATPase was further purified on a Sepharose 6B column equilibrated and eluted with a buffer containing 20 mM Tricine/NaOH, 1 mM ATP, 2 mM EDTA, and 0.1 mM DTT at pH 8.0. The purified enzyme was precipitated by 50% saturated ammonium sulfate and stored at 4 °C. The enzyme purity was greater than 95% as judged by SDS–polyacrylamide gel electrophoresis (Laemmli, 1970).

Ammonium sulfate precipitated CF_1 was desalted by passage through a Sephadex G-50 centrifuge column (Penefsky, 1979) equilibrated in 50 mM Tris-HCl, pH 8.0. In experiments requiring activated enzyme, the recovered enzyme was made 50 mM in DTT by addition of solid DTT and was incubated for 90 min at room temperature (Devlin, 1989). The DTT was then removed by passage through another Sephadex centrifuge column equilibrated with the Tris-HCl buffer.

Assays. Ca^{2+} ATPase activity was routinely measured as P_i formation in an assay mixture of 32 mM Tricine/NaOH, 8 mM $CaCl_2$, and 3.2 mM ATP, pH 8.0 at 37 °C. Protein determinations were performed by the method of Lowry et al. (1951) with bovine serum albumin as a standard.

Kinetic Studies. Reaction mixtures for ATPase activity contained, in a 0.4-mL total volume, 200 mM Tris-HCl (pH 8.0), 10 mM $CaCl_2$, and 0.4–30 mM [γ-^{32}P]ATP (containing approximately 10^7 cpm/mL). In experiments where the cobalt–nucleotide complex was used as an inhibitor of the ATPase activity, the complex was added immediately before the reaction was started by the addition of CF_1. Reaction mixtures were incubated at 37 °C for 10 min. Following this incubation, 100-μL aliquots of the reaction mixture were added to tubes containing 800 μL of a mixture of 2.8% $HClO_4$, 0.625 mM phosphate buffer, pH 6.9, and 1.25% ammonium molybdate/1 N H_2SO_4. The complexed phosphate was extracted into 1 mL of a 1:1 (v/v) mixture of water-saturated isobutyl alcohol and benzene, and 0.4 mL of the organic phase was counted on a Beckman LS 8000 liquid scintillation counter. Controls were treated identically but received no $CaCl_2$. Rates of ATPase activity were determined to be approximately 30–37 μmol of ATP hydrolyzed (mg of CF_1)$^{-1}$ min^{-1} in 20 mM Tris-HCl, pH 8.0, 10 mM $CaCl_2$, and 10 mM [γ-^{32}P]ATP.

Data Analysis for Kinetic Measurements. The kinetic data were fit to

$$v_i = \frac{V[S_i]}{[S_i] + K_M(1 + [I]/K_{is} + [Ca]_f/K_{iCa})}(1 + \epsilon_i) \qquad (1)$$

for competitive inhibition where v_i is the experimentally determined rate at substrate concentration $[S_i]$ in the presence of both inhibitors, [I] is the concentration of Co$(NH_3)_4$AMPPCP, $[Ca]_f$ is the concentration of free divalent calcium ions, K_{iCa} is the inhibition constant of $[Ca]_f$ on the ATPase (Hochman & Carmeli, 1981), and K_{is} is the apparent inhibition constant of Co$(NH_3)_4$AMPPCP on the ATPase. The variance in the rate is ϵ_i. The data were analyzed to minimize $\sum\epsilon_i^2$. Attempts were also made to fit the data to the equation for noncompetitive inhibition by I:

$$v_i = \frac{V[S_i]}{K_M(1 + [I]/K_{is} + [Ca]_f/K_{iCa}) + [S](1 + [I]/K_{is})} \times (1 + \epsilon_i) \qquad (2)$$

Solutions. All glassware and plasticware was treated with 0.1 M HCl and 1 mM EDTA and thoroughly washed with distilled, deionized water. This stringent washing procedure was employed to minimize the concentration of contaminating paramagnetic ions within the NMR sample. All stock solutions, except the ATPase and $MnCl_2$, were rigorously treated

with Chelex 100 to remove divalent cations. Co$(NH_3)_4$AMPPCP solutions were stored at −20 °C, while the ATPase and all other stock solutions were stored at 4 °C. Stock D_2O, Tris-d_{11}, and Co$(ND_3)_4$AMPPCP were prepared as previously described (Stewart, 1988). Generally, sample volumes were 100 μL for PRR experiments, 1.4 mL for ^{31}P NMR experiments, and 0.6 mL for ^1H NMR experiments unless otherwise stated.

Enzyme Preparation for PRR and ^{31}P NMR Experiments. Ammonium sulfate precipitated enzyme was centrifuged at 5000*g* for 20 min at 25 °C to pellet the enzyme. From this point on, the activation procedure was the same as that described above, except that the Penefsky column treatment prior to DTT addition was omitted. After the Lowry assay was performed, the sample was concentrated on a Centricon-30 if necessary.

Enzyme Preparation for ^1H NMR Experiments. After the ammonium sulfate precipitated enzyme was pelleted (as described above), it was resuspended in 40 mM Tris-d_{11} in D_2O, pD 8.0, and activated by addition of DTT to a concentration of 50 mM for 90 min. The sample was then concentrated 10-fold in a Centricon-30 microconcentrator, homogenized in 40 mM Tris-D_{11} in D_2O, pD 8.0, and passed through a Penefsky column in the same buffer. In order to remove H_2O from the sample, the enzyme was diluted and reconcentrated twice more with fresh, deuterated Tris-d_{11} buffer before use.

NMR Measurements. All water proton NMR measurements were performed on a variable-frequency pulsed NMR spectrometer of our own design. The magnet for this spectrometer is a Varian 4012A electromagnet with a 2100-B power supply, which has been modified for solid-state operation. The rf components and the pulse programmer were designed and built by SEIMCO, New Kensington, PA, and the frequency source was a Harris PRD 7838 frequency synthesizer. All measurements were obtained at a probe temperature of 23 ± 2 °C. Spin–lattice relaxation times (T_1) were measured with an inversion–recovery pulse sequence $(180°-\tau-90°-5T_1)_n$. T_1 values were calculated from

$$T_1 = \tau(\text{null})/\ln 2 \quad (3)$$

The paramagnetic contribution to the relaxation rate ($1/T_{1p}$) was calculated as the difference between the observed relaxation rate for an enzyme or enzyme–ligand solution in the presence of Mn^{2+} [$1/T_{1(obs)}$] and the relaxation rate measured for the same complex in the absence of Mn^{2+} [$1/T_{1(o)}$]:

$$1/T_{1p} = 1/T_{1(obs)} - 1/T_{1(o)} \quad (4)$$

The observed enhancement values (ϵ^*) were calculated as the ratio of $1/T_{1p}$ measured for an enzyme–Mn^{2+} or enzyme–Mn^{2+}–ligand solution ($1/T_{1p}^*$) to $1/T_{1p}$ measured for the same Mn^{2+} or Mn^{2+}–ligand solution without enzyme ($1/T_{1p}^o$) (Eisinger, 1962):

$$\epsilon^* = \frac{1/T_{1p}^*}{1/T_{1p}} = \frac{1/T_{(obs)}^* - 1/T_{1(o)}^*}{1/T_{(obs)} - 1/T_{1(o)}} \quad (5)$$

where the asterisk (*) denotes the presence of enzyme. The observed enhancement (ϵ^*) of a solution is the sum of the individual enhancements of each species in the solution (Mildvan & Engle, 1972):

$$\epsilon^* = \sum \chi_i \epsilon_i \quad (6)$$

where χ_i is the mole fraction of the ith species and ϵ_i is the enhancement due to the ith species. PRR titration curves were best fit with a computer program, REED3, adapted from a program kindly provided by Dr. George H. Reed, Institute for Enzyme Research, University of Wisconsin, Madison, WI,

Scheme I

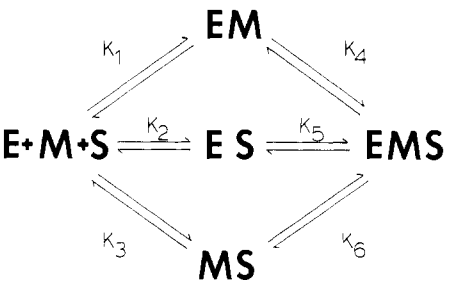

which uses a Marquardt algorithm for the solution of simultaneous linear equations. The equilibria involved are those shown in Scheme I. The algorithm employed has been previously described (Reed et al., 1970). In the fitting procedure, a known (literature) value is used for K_3, and assumptions are made initially for K_1, K_2, K_4, K_5, and K_6. REED3 then solves the conservation equations for metal, substrate, and enzyme and the dissociation constant equations for the six equilibria shown in Scheme I to obtain best fits for K_1, K_2, K_4, K_5, and K_6 and best-fit equilibrium concentrations for free metal, substrate, and enzyme and also the complexes EM, ES, MS, and EMS (Scheme I). These values are used to fit the enhancement equations (eq 6), best-fit values for ϵ_{EM} and ϵ_{EMS} being used. This procedure accounts for all free and bound Mn^{2+} species shown in Scheme I.

Phosphorus-31 NMR spectra and longitudinal relaxation times (T_1) were obtained at 145.1 MHz on a Nicolet Magnetics Corp. NT-360/Oxford spectrometer equipped with a 1200/293B data system and at 121.7 MHz on a General Electric QN-300 spectrometer. The spectra were measured at 23 ± 1 °C with a 10-mm phosphorus probe and an internal deuterium lock. The 90° pulse width was typically 25–30 μs at 145.1 MHz and 23–26 μs at 121.7 MHz. Uninterrupted, incoherent proton decoupling at low levels (less than or equal to 0.7 W) was employed. Chemical shifts were referenced to 0.4 M phosphoric acid. The samples typically contained 5 μM DTT-activated enzyme, 15 mM CoAMPPCP, 40 mM Tris-HCl, pH 8.0, bubbled with O_2 for 2 min to prevent breakdown of Co^{3+} to Co^{2+}, and 60–70% D_2O. After extended NMR measurements (15–17 h), the enzyme was found to retain more than half its activity, and no systematic changes were observed during the NMR experiments.

Proton NMR spectra were also obtained at two frequencies: at 300 MHz on a General Electric QN-300 spectrometer and at 361 MHz on a Nicolet Magnetics Corp. NT-360/Oxford spectrometer. The spectra were measured at 25 ± 1 °C with a 5-mm proton probe and deuterium lock. The 90° pulse width was typically 11.5 μs at 300 MHz and 9.75 μs at 361 MHz. The HDO signal was decoupled during delays prior to the pulse sequences.

Longitudinal relaxation times were determined from an optimized inversion–recovery experiment (Craik & Levy, 1984). Typically, eight τ values were used in the $180°-\tau-90°$ sequence for ^{31}P NMR measurements, and 18–24 τ values were used in ^1H NMR experiments. T_1 values and their standard deviations were calculated with a three-parameter fit to the data. This fitting routine corrects for inhomogeneities in the H_1 field that produce incomplete inversion during the 180° pulse (Levy & Peat, 1975). For ^{31}P NMR experiments, 160–200 accumulations of 8K data points were collected per τ value, while only 16 accumulations of 8K data points were collected for the ^1H NMR experiments.

Paramagnetic contributions to the longitudinal relaxation rates of the proton and phosphorus nuclei of Co-

$(NH_3)_4$AMPPCP were calculated with a computer program, RCALC (Devlin, 1989), which allows one to vary the number of tight and weak metal binding sites in order to best fit the experimental data.

Conformational analysis was done on a Silicon Graphics workstation using the program MMS (Copyright UCSD). $Co(NH_3)_4$AMPPCP was constructed from the X-ray diffraction data of rubidium adenosine 5'-diphosphate monohydrate (Viswamitra et al., 1976) and $Co(NH_3)_4H_2P_3O_{10}$ (Merritt et al., 1978) as described by Stewart (1988), corrected for the exchange of methylene for oxygen in AMPPCP. The conformation of the enzyme-bound CoAMPPCP was then determined with the distances calculated from the NMR data.

Theory. Calculations of Mn^{2+}–phosphorus and Mn^{2+}–proton distances are based on the theory of Solomon and Bloembergen (Solomon, 1955; Solomon & Bloembergen, 1956; Bloembergen, 1957; Bernheim et al., 1959) for the paramagnetic effects on the nuclear spin relaxation rates of a magnetic nucleus that is bound near a paramagnetic species. In general, the paramagnetic contribution to the longitudinal relaxation rate, $1/T_{1p}$ is described by

$$1/fT_{1p} = q/(T_{1M} + \tau_M) + 1/T_{1(os)} \quad (7)$$

where f is the ratio of the concentration of paramagnetic ion to the concentration of ligand, q is the number of ligands in the first coordination sphere of the paramagnet, T_{1M} is the relaxation time in the first coordination sphere of the paramagnet, τ_M is the residence time of the ligand in the first coordination sphere, and $1/T_{1(os)}$ is the outer-sphere contribution to the relaxation rate.

In the limit of fast exchange, when the rate of chemical exchange of the ligand between the coordination sphere and the bulk solvent is faster than the rate of relaxation in the first coordination sphere (i.e., when $1/\tau_M \gg 1/T_{1M}$), and assuming outer-sphere contributions are negligible, eq 7 reduces to

$$1/fT_{1p} = q/T_{1M} \quad (8)$$

For the water proton relaxation experiments, eq 8 becomes

$$1/fT_{1p} = 2[H_2O]/[Mn^{2+}]_bT_{1p} \quad (8a)$$

For the high-resolution NMR experiments, eq 8 becomes

$$1/fT_{1p} = [Co(NH_3)_4AMPPCP]/[Mn^{2+}]_bT_{1p} \quad (8b)$$

where $[Mn^{2+}]_b$ is the concentration of enzyme-bound Mn^{2+}.

The Solomon–Bloembergen equations that describe the dipolar Mn^{2+}–phosphorus and Mn^{2+}–proton interactions, respectively, are

$$r^6 = (601)^6T_{1M}f(\tau_c) \quad (9)$$

$$r^6 = (812)^6T_{1M}f(\tau_c) \quad (10)$$

where r is the internuclear distance and

$$f(\tau_c) = \frac{3\tau_c}{1 + \omega_I^2\tau_c^2} + \frac{7\tau_c}{1 + \omega_S^2\tau_c^2} \quad (11)$$

where ω_I and ω_S are the nuclear and electronic Larmor frequencies, respectively. τ_c is known as the dipolar correlation time and characterizes the process that modulates the dipolar interaction. In turn, it is described as a function of three time constants by

$$1/\tau_c = 1/\tau_r + 1/\tau_s + 1/\tau_m \quad (12)$$

τ_r characterizes the rotation of the internuclear ion–nucleus radius vector. τ_s is the electron spin relaxation time. τ_m is the residence time of the nuclear species in the first coordination sphere of the paramagnet. The smallest time constant determines τ_c.

Results

Steady-State Kinetics of Competition between Co$(NH_3)_4$AMPPCP and CaATP. Steady-state kinetic studies were performed to characterize the interaction of Co$(NH_3)_4$AMPPCP with CF_1. Dixon plots of the inhibition of ATPase activity by $Co(NH_3)_4$AMPPCP, corrected for additional inhibition by free Ca^{2+}, were consistent with competitive inhibition by $Co(NH_3)_4$AMPPCP against CaATP (eq 1). Assuming a value of 7 mM for K_{iCa} in eq 1 (Hochman & Carmeli, 1981) and a value of 10 mM for K_M yields a best-fit value of K_i for $Co(NH_3)_4$AMPPCP of 0.65 mM on the DTT-activated ATPase. Similar results have been obtained (with a K_i of 0.724 mM) for β,γ-bidentate CrATP (Frasch & Selman, 1982). Determination of the inhibition constant for MnATP proved difficult due to the extreme inhibition caused by free Mn^{2+} (Hochman & Carmeli, 1981).

Water Proton Relaxation Rate Titrations with Substrates. The role of Mn^{2+} with the CF_1 ATPase–Mn^{2+} and CF_1 ATPase–Mn^{2+}–substrate complexes was investigated by measurement of water proton nuclear relaxation rate enhancements (PRR). In order to characterize the binding of substrate to the enzyme–metal complex, the change in enhancement upon addition of substrate to the binary complex to form the metal–enzyme–substrate, or ternary, complex was measured. In these experiments, Mn^{2+} was used as a probe for divalent metal sites, and a number of substrates and substrate analogues were employed to examine different intermediate complexes. Complexes of Co(III) [and Cr(III)] with ATP, ADP, and other nucleotides have been found to be effective analogues of Mg^{2+}- and Mn^{2+}–nucleotide complexes in many enzymes, including the ATPases (Grisham, 1988). Methylene-ATP, or AMPPCP, is a useful analogue of ATP which is strictly unhydrolyzable by ATPases and kinases (Yount, 1975). No hydrolysis of $Co(NH_3)_4$AMPPCP was observed in solutions of the CF_1 ATPase in these studies.

Titrations of the latent CF_1 ATPase–Mn^{2+} complex with P_i, ADP, ATP, $Co(NH_3)_4$ADP, and $Co(NH_3)_4$ATP are shown in Figure 1. Figure 2 shows the effect of ADP, ATP, vanadate, $Co(NH_3)_4$ATP, and $Co(NH_3)_4$AMPPCP on the enhancement of water proton relaxation by Mn^{2+} bound to the DTT-activated CF_1 ATPase. In all these experiments, the solutions contained 1:1 ratios of Mn^{2+} and ATPase, conditions that promote Mn^{2+} binding to the high-affinity sites described by Hochman and Carmeli (1981) but not the low-affinity sites described by the same authors. Because the change in proton relaxation rate enhancement upon substrate binding reflects changes in the coordination sphere of the enzyme-bound paramagnet, plots of enhancement (ϵ^*) versus added substrate correlate directly with substrate binding to the binary complex.

For all substrates and substrate analogues except vanadate, titration of the binary E–Mn complex with the substrate (S) caused an increase in the observed water proton relaxation enhancement, consistent with the formation of ternary E–Mn–S complexes. Changes in the observed enhancement such as observed here can arise from a variety of factors. In most substrate titrations of binary complexes in other enzyme systems, the number of water ligands coordinated to Mn^{2+} decreases as the substrate binds to the metal, while other factors do not change appreciably, leading to a decrease in the observed enhancement. Conditions that would lead to an increased observed enhancement include (a) an increase in the number of water ligands coordinated to Mn^{2+}, q, (b) an increase in the exchange rate of water molecules into the first

Table I: Analysis of Frequency Dependence of T_{1p} for Latent and DTT-Activated CF_1

complex	τ_c ($s \times 10^9$)[a]	frequency (MHz)	$1/fT_{1p}$ ($s^{-1} \times 10^{-6}$)	$f(\tau_c)$ ($s \times 10^9$)	q
latent CF_1					
ATPase–Mn^{2+}	2.6	45	7.21	5.1	2.3
ATPase–Mn^{2+}–ADP	3.5	45	7.39	5.3	2.3
ATPase–Mn^{2+}–P_i	2.5	45	7.02	5.0	2.3
ATPase–Mn^{2+}–ATP	4.1	45	5.44	5.2	1.7
DTT-activated CF_1					
ATPase–Mn^{2+}	3.7	49	2.61	4.8	0.9
ATPase–Mn^{2+}–ADP	3.7	49	4.46	4.8	1.5
ATPase–Mn^{2+}–ATP	4.5	49	3.80	4.6	1.4
ATPase–Mn^{2+}–AMPPCP	5.2	49	4.27	4.4	1.6
ATPase–Mn^{2+}–CoAMPPCP	4.5	49	4.04	4.6	1.4

[a] Correlation times were determined from plots similar to Figure 3. In these plots, the slope of the plot of T_{1p} versus ω_I^2 divided by the y intercept is τ_c^2. The function $f(\tau_c)$ is calculated from eq 11, r is 2.87 Å [from crystallographic data of Reuben and Cohn (1970)], and q is calculated from eqs 8 and 10.

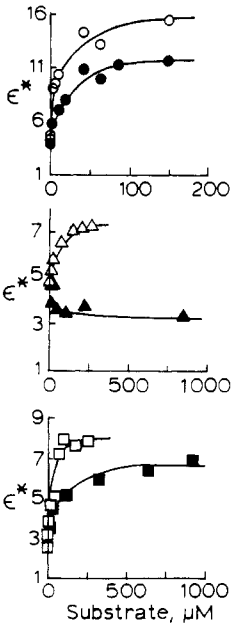

FIGURE 1: Effects of substrates and substrate analogues on the enhancement of water proton relaxation by Mn^{2+} bound to the latent CF_1 ATPase. Titrants were ADP (○), ATP (●), P_i (△), VO_4^{3-} (▲), $Co(NH_3)_4ADP$ (□), and $Co(NH_3)_4ATP$ (■). Conditions were as described under Experimental Procedures and included 0.005 mM ATPase, 0.005 mM Mn^{2+}, and 50 mM Tris-HCl, pH 8.0.

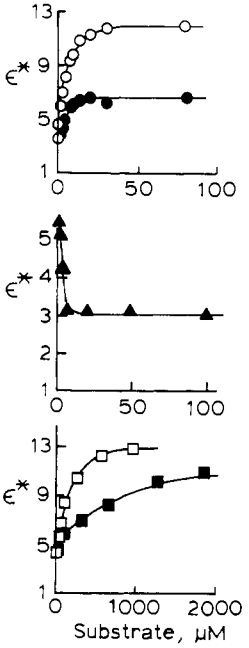

FIGURE 2: Effects of substrates and substrate analogues on the enhancement of water proton relaxation by Mn^{2+} bound to the DTT-activated CF_1 ATPase. Titrants were ADP (○), ATP (●), VO_4^{3-} (△), $Co(NH_3)_4ATP$ (□), and $Co(NH_3)_4AMPPCP$ (■). Conditions were as described under Experimental Procedures and included 0.005 mM DTT-activated ATPase, 0.005 mM Mn^{2+}, and 50 mM Tris-HCl, pH 8.0.

coordination sphere of the paramagnet, (c) an increase in the correlation time for the water–Mn^{2+} interactions, or (d) an increase in Mn^{2+} bound to the enzyme upon addition of substrate. Choosing among these possibilities requires an estimate of the dipolar correlation time for the Mn–H_2O interaction in each complex, and this can be obtained most conveniently by a study of the frequency dependence of proton relaxation.

Frequency Dependence of $1/T_{1p}$ of Water on Enzyme-Bound Mn^{2+}. In order to (a) determine whether the correlation time, τ_c, for H_2O–Mn^{2+} interactions exhibited large changes with added titrant and (b) use the relaxation data from these studies to determine distances and coordination numbers at the active site, a study of the frequency dependence of relaxation was carried out. Figure 3 shows a plot of T_{1p} versus ω_I^2 for the DTT-activated ATPase binary and ternary complexes. Similar data were obtained for the latent ATPase complexes (data not shown). The relaxation rate shows a frequency dependence for all complexes, consistent with the formation of stable macromolecular intermediates. A summary of the data for both latent and DTT-activated CF_1 complexes is presented in Table I. For the latent CF_1 complex, τ_c is 2.6×10^{-9} s for the binary complex and ranges from 2.5×10^{-9} to 4.1×10^{-9} s for the ternary complexes. The τ_c

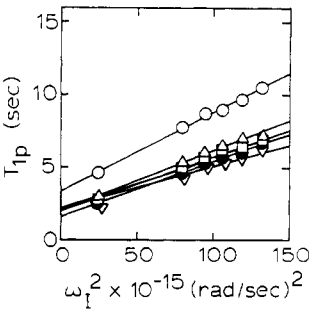

FIGURE 3: Frequency dependence of the paramagnetic contribution to the relaxation rate ($1/T_{1p}$) of water protons for complexes of Mn^{2+}, the DTT-activated CF_1 ATPase (○), and the following substrates: 0.024 mM ATP (△), 1.7 mM $Co(NH_3)_4AMPPCP$ (□), 0.032 mM AMPPCP (●), or 0.122 mM ADP (▽). All solutions contained 50 mM Tris, pH 8.0, 0.005 mM DTT-activated CF_1, and 0.005 mM $MnCl_2$.

values are similar for the activated CF_1 complex; i.e., τ_c is 3.7 $\times 10^{-9}$ s for the binary complex and ranges from 3.7×10^{-9} to 5.2×10^{-9} s for the ternary complexes. However, the number of fast-exchanging water molecules in the first coordination sphere of the paramagnetic ion in the binary E–Mn

Table II: Binding of Nucleotides and Substrates to CF_1 ATPase

complex	best-fit values of constants from Scheme I[a,b]						
	K_1 (μM)	K_2 (μM)	K_3 (μM)	K_4 (μM)	K_5 (μM)	ϵ_{EM}	ϵ_{EMS}
latent CF_1 complex							
Mn-E-P_i	0.95	140		56.0	0.38	6.0	11.0
Mn-E-ADP	4.70	13		1.3	0.13	6.5	22.0
Mn-E-ATP	6.00	120		5.0	0.25	6.5	26.0
Mn-E-vanadate	6.00	140		8.8	0.38	11.0	4.0
Mn-E-Co$(NH_3)_4$ADP	14.0	665		57.0	1.20	10.0	22.0
Mn-E-Co$(NH_3)_4$ATP	6.75	665		375.0	3.80	10.0	22.0
DTT-activated CF_1 complex							
Mn-E-ADP	8.0	42		3.3	0.64	15.0	22.0
Mn-E-ATP	6.0	80		4.0	0.30	10.0	10.5
Mn-E-vanadate	6.0	140		8.8	0.38	11.0	3.0
Mn-E-Co$(NH_3)_4$ATP	6.75	3210		137.4	0.29	13.0	22.0
Mn-E-Co$(NH_3)_4$AMPPCP	6.75	3210		209.0	0.44	15.0	22.0
literature values[c]							
E-Mn	3.8[d]						
E-Mn	14.7[e]						
E-Mn	11.2[f]						
Mn-ADP		100[g]					
Mn-ATP		14[g]					
Mn-CoATP		15 000[h]					
Mn-P_i		4 700[i]					
Mg-E-ADP			3.75[j]				
Mg-E-ATP			2.90[k]				
Mg-E-AMPPNP			7.0[l]				
E-ADP-Mn				0.83[d]			
E-ATP-Mn				0.98[d]			

[a] K_D values determined in titrations with indicated [ligand]. Errors in these values are ±3% due to fitting uncertainties and ±8% due to errors in the water proton relaxation data. [b] For definition of K_1, K_2, K_3, K_4, K_5, refer to Scheme I. [c] K_3 values from indicated references were used for the fitting program (REED3). K_1, K_4, and K_5 literature values are provided here for purposes of comparison. [d] Hochman & Carmeli, 1981. [e] Hiller & Carmeli, 1985. [f] Haddy et al., 1985. [g] Mildvan & Cohn, 1966. [h] Stewart & Grisham, 1988. [i] Benkovic et al., 1972. [j] Cantley & Hammes, 1975. [k] Bruist & Hammes, 1981. [l] Frasch & Sharp, 1985.

complex is different for the latent versus the activated enzyme (2.3 vs 0.9). The number of fast-exchanging water molecules bound to Mn^{2+} in the DTT-activated enzyme increases slightly (from 0.9 to approximately 1.5) upon formation of ternary complexes with substrates and substrate analogues. Values of q for the latent enzyme binary and ternary complexes were similar (1.7–2.3). The values of q for the ternary E–Mn–ATP complexes of latent and activated CF_1 were indistinguishable (1.7 vs 1.4), but the q values for the E–Mn–ADP complexes differed significantly (2.3 for the latent enzyme complex and 1.5 for the activated enzyme complex).

Analysis of Binding Constants for Substrates and Metals to CF_1. Using the model for EMS binding shown in Scheme I, the observed enhancement titration data were employed to determine best-fit values of K_4 (K_{EMS}) and the other binding constants with a computer program, REED3, which takes into account all complexes of Mn^{2+} and relevant equilibrium constants. The fitted values for K_1, K_2, K_4, K_5, and relevant equilibrium constants from the literature are shown in Table II. Table II shows that there is a dramatic tightening of metal binding in the presence of substrate (i.e., $K_5 < K_1$) for both latent and DTT-activated enzyme. In addition, K_4 is considerably less than K_2 for all ternary complexes. ADP and ATP exhibit tight binding to both the latent and activated CF_1–Mn^{2+} complexes. As in a number of other enzyme systems (Macara, 1980), vanadate binds more tightly than phosphate to the EM complex. All three Co(III) complexes exhibit weak binding to the EM complex compared to ATP and ADP. It should be noted that the best-fit K_D values determined for Mn^{2+} binding (K_1 and K_5) agree well with those determined by numerous other workers for a class of high-affinity Mn^{2+} sites on CF_1 [notably, Hochman and Carmeli (1981)].

^{31}P NMR Studies of the Ternary Mn^{2+}–ATPase–Co$(NH_3)_4$AMPPCP Complex. ^{31}P NMR relaxation rates were measured in solutions of Mn^{2+} and DTT-activated CF_1 ATPase at 121.7 and 145.1 MHz. The spectra (Figure 4) consist of superimposed resonances for both the Λ and Δ diastereomers of Co$(NH_3)_4$AMPPCP. However, the P_α, P_β, and P_γ resonances are clearly resolved. The assignment of the Δ and Λ diastereomers of Co$(NH_3)_4$AMPPCP is still under investigation in our laboratory. The Λ isomer of the metal–nucleotide complex has been proposed as the substrate for the CF_1 ATPase (Frasch & Selman, 1982).

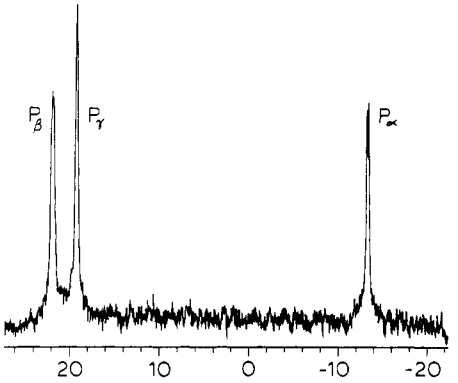

FIGURE 4: Phosphorus-31 nuclear magnetic resonance spectrum of Co$(NH_3)_4$AMPPCP at 121.7 MHz, pH 8.0, 24 °C. Chemical shifts are relative to 0.4 M phosphoric acid. The solution contained D_2O (60%) for field/frequency locking.

The presence of CF_1 ATPase causes a 4–6-fold enhancement of the effect of Mn^{2+} on the ^{31}P relaxation rates of Co$(NH_3)_4$AMPPCP, establishing the formation of a ternary Mn^{2+}–ATPase–Co$(NH_3)_4$AMPPCP complex. Under the solution conditions employed, both binary Mn^{2+}–Co$(NH_3)_4$AMPPCP and ternary Mn^{2+}–ATPase–Co$(NH_3)_4$AMPPCP were present in these NMR studies. Subtraction of the contributions to the observed $1/T_{1p}$ from the binary Mn^{2+}–Co$(NH_3)_4$AMPPCP complex (Devlin, 1989)

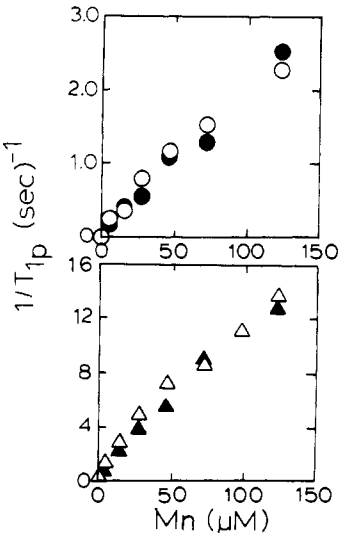

FIGURE 5: Effect of Mn^{2+} on longitudinal relaxation rates of the α- (●, ○), β- (△), and γ- (▲) phosphorus nuclei of $Co(NH_3)_4AMPPCP$ in the presence of DTT-activated CF_1 ATPase. The solution contained 5 μM DTT-activated CF_1, 15 mM CoAMPPCP, 40 mM Tris, pH 8.0, and D_2O (60%) for locking.

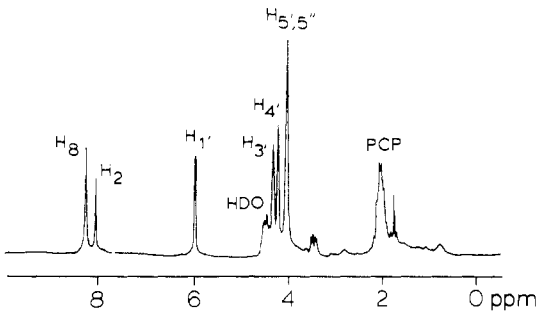

FIGURE 6: Hydrogen-1 nuclear magnetic resonance spectrum of $Co(ND_3)_4AMPPCP$ at 300 MHz, pH 8.0, 25 °C. Chemical shifts are relative to DSS. The solution contained D_2O (99+%), and the residual HDO signal was reduced by irradiation with the decoupler during the 180° pulse and during all pulse delays.

yielded the contribution to $1/T_{1p}$ from the ternary Mn^{2+}–ATPase–$Co(NH_3)_4AMPPCP$ complex, as shown in Figure 5. As will be discussed in the next section, the paramagnetic effects of Mn^{2+} in Figure 5 include effects from Mn^{2+} at two different classes of noninteracting metal sites on the enzyme. In separate experiments, the addition of saturating amounts of diamagnetic Mg^{2+} ion produced no measurable increase in the relaxation rates of the phosphorus nuclei of $Co(NH_3)_4AMPPCP$, indicating that the effects of added Mn^{2+} are due entirely to electron–nuclear dipolar interactions.

^1H NMR Studies of the Ternary Mn^{2+}–ATPase–$Co(NH_3)_4AMPPCP$ Complex. ^1H NMR relaxation rates of the protons of $Co(NH_3)_4AMPPCP$ were measured in solutions of Mn^{2+} and DTT-activated CF_1 ATPase at 300 and 361 MHz. The 300-MHz ^1H NMR spectrum of $Co(ND_3)_4AMPPCP$ at 25 °C is shown in Figure 6. The resonances are labeled in the conventional manner. In this particular sample, $Co(NH_3)_4AMPPCP$ was dissolved in 99.8% D_2O, and the amine protons were exchanged for deuterium ligands. The residual HDO signal, which is partially irradiated to reduce its intensity, appears at 4.75 ppm relative to DSS. All NMR experiments were performed at room temperature to ensure enzyme stability. An unfortunate drawback of the use of this temperature is that at temperatures above 15 °C the HDO resonance obscures the ribose $H_{2'}$ resonance at 300 MHz (Stewart, 1988).

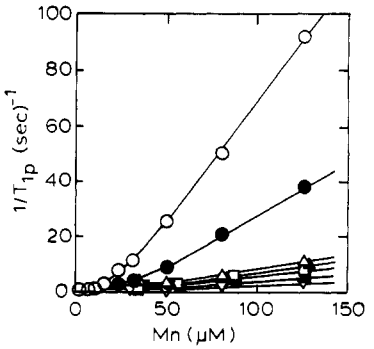

FIGURE 7: Effect of Mn^{2+} on the longitudinal relaxation rates of proton nuclei of $Co(NH_3)_4AMPPCP$ in the presence of DTT-activated CF_1 ATPase. Solutions contained 10 μM DTT-activated CF_1, 10 mM CoAMPPCP, and 40 mM Tris, pH 8.0. Data are shown for the H_8 (○), PCP (●), H_2 (△), $H_{3'}$ (▲), $H_{5',5''}$ (□), $H_{1'}$ (■), and $H_{4'}$ (▽) protons.

Table III: Mn^{2+}–P Distances in the ATPase–Mn^{2+}–$Co(NH_3)_4AMPPCP$ Complex[a,b]

	$1/fT_{1p}$ (s^{-1})		Mn–P distance (Å) (±14%)[d]	
nucleus[c]	site 1	site 2	site 1	site 2
α_1	703	6500	7.1 (7.7)	4.9 (5.4)
α_2	834	8350	6.9 (7.6)	4.7 (5.2)
β	2620	29900	5.7 (6.2)	3.8 (4.2)
γ	4060	25600	5.3 (5.8)	3.9 (4.3)

[a] Calculated with $\tau_c = 1.0 \times 10^{-9}$ s (from frequency study). [b] The values are calculated with eq 9 assuming two classes of noninteracting metal binding sites with $K_1 = 0.98$ μM and $K_2 = 50.0$ μM (Hochman & Carmeli, 1981) (Table I). The first numbers shown in each row assume one tight metal binding site and one weak metal binding site, respectively. The numbers in parentheses assume three tight sites and three weak sites. All numbers are the average distance values of four separate experiments, two at 121.7 MHz and two at 145.1 MHz. [c] The subscripts denote the Δ and Λ diastereomers of $Co(NH_3)_4AMPPCP$, which are currently being assigned in our laboratory. [d] The estimate of error in these values is based primarily on the error in the estimation of τ_c.

Table IV: Mn^{2+}–H Distances in the ATPase–Mn^{2+}–$Co(NH_3)_4AMPPCP$ Complex[a,b]

H	$1/fT_{1p}$ (s^{-1})		Mn–H distance (Å) (±14%)[c]	
nucleus	site 1	site 2	site 1	site 2
H_8	982	53800	7.6 (7.9)	3.9 (4.3)
H_2	149	6830	10.4 (10.9)	5.5 (6.1)
$H_{1'}$	214	3330	9.8 (10.4)	6.2 (6.9)
$H_{3'}$	214	4480	9.8 (10.9)	5.9 (6.6)
$H_{4'}$	133	1910	10.6 (11.3)	6.8 (7.6)
$H_{5'}$	274	3670	9.4 (10.1)	6.1 (6.7)
H_{pcp}	778	20000	7.9 (8.4)	4.6 (5.1)

[a] Calculated with $\tau_c = 1.023 \times 10^{-9}$ s (from frequency study). [b] The values are calculated with eq 10 assuming two classes of noninteracting metal binding sites with $K_1 = 0.98$ μM and $K_2 = 50.0$ μM (Hochman & Carmeli, 1981) (Table I). The first numbers shown in each row assume one tight metal binding site (site 1) and one weak metal binding site (site 2), respectively. The numbers in parentheses assume three tight sites and three weak sites. All numbers are the average distance values of multiple experiments performed at 300.5 MHz. [c] The estimate of error in these values is based primarily on the error in the estimation of τ_c.

As shown in Figure 7, addition of Mn^{2+} to solutions of DTT-activated CF_1 ATPase and $Co(NH_3)_4AMPPCP$ results in increases in $1/T_1$ for all seven proton resonances of the nucleotide analogue. The titrations of several of the proton resonances are noticeably biphasic, consistent with an ordered binding of Mn^{2+} to tight and weak metal sites on the enzyme (Hochman & Carmeli, 1981), each exhibiting a different interaction with the bound substrate nuclei. At low levels of added Mn^{2+} (0–10 μM), linear increases in $1/T_1$ with Mn^{2+} are observed. The normalized slopes of these plots are reported

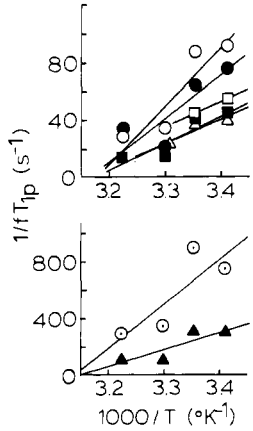

FIGURE 8: Temperature dependence of $1/fT_{1p}$ for the H_2 (○), $H_{1'}$ (■), $H_{3'}$ (□), $H_{4'}$ (△), $H_{5',5''}$ (●), H_8 (⊙), and PCP (▲) nuclei of $Co(NH_3)_4AMPPCP$ (10 mM) in the presence of 10 μM DTT-activated CF_1 and 125 μM $MnCl_2$. The solution contained 40 mM Tris, pH 8.0, and 99+% D_2O. All values of $1/fT_{1p}$ are corrected for effects in the absence of enzyme.

as $1/fT_{1p}$ values for each proton of the substrate in Table IV. The paramagnetic effect of low levels of Mn^{2+} was 7-fold greater for the H_8 proton of the bound substrate than for the $H_{4'}$ proton. At higher levels of Mn^{2+}, the observed relaxation rates are even more sensitive to added Mn^{2+}, consistent with binding of Mn^{2+} to a second class of sites. The relative effects of high levels of Mn^{2+} on the protons of the substrate were different from those at low Mn^{2+}. Thus, the paramagnetic effect of high Mn^{2+} on the H_8 proton of the bound substrate was approximately 28-fold larger than that on the $H_{4'}$ proton. The relative magnitudes of the increase reflect the degree of interaction of each of the protons of $Co(NH_3)_4AMPPCP$ with bound Mn^{2+}. Thus, for example, it is clear from the data in Figure 8 that the H_8 and H_{pcp} protons experience the greatest interaction with the Mn^{2+} at the active site. Two classes of Mn^{2+} binding sites have been characterized by other researchers (Hochman & Carmeli, 1981) using EPR measurements. Our relaxation data were best fit with their dissociation constants for the one tight site (K_d = 3.5 ± 2.5 μM) and one weak site (K_D = 50 ± 25 μM in most enzyme–Mn^{2+} nucleotide complexes). The best-fit K_D values for the tight Mn^{2+} site are in excellent agreement with the best-fit values for K_1 and K_5 in Table II, which were obtained from the water proton relaxation measurements. The good agreement between the best-fit K_D values for the water proton relaxation studies, the high-resolution ^{31}P and ^1H NMR data, and the tight sites characterized by Hochman and Carmeli (1981) is consistent with the notion that the high-resolution ^1H and ^{31}P NMR data are describing the same sites observed in the PRR experiments and reported earlier by Hochman and Carmeli (1981). Tables III and IV list the paramagnetic contributions to relaxation rates of the phosphorus and proton nuclei of $Co(NH_3)_4AMPPCP$ in the ternary complex. The high- and low-affinity Mn^{2+} sites are henceforth referred to as site 1 and site 2, and the paramagnetic effects of high and low levels of Mn^{2+} are distinguished in this manner in Tables III and IV. Effects ascribed to the two sites were resolved with the RCALC program described under Experimental Procedures and with the dissociation constants of Hochman and Carmeli (1981) and, in the case of site 1, the dissociation constants obtained from the water relaxation data (Table II). As was the case for the data shown in Figure 5, contributions to the observed relaxation rates from the binary Mn^{2+}–$Co(NH_3)_4AMPPCP$ complex were subtracted from the observed $1/T_1$ values to yield the data shown in Figure 7.

Determination of Correlation Times and Distances in the Ternary Complex. In order to use the data of Figures 5 and 7 to calculate the distances between Mn^{2+} and the phosphorus and proton nuclei of $Co(NH_3)_4AMPPCP$ in the ternary complex, it was necessary to determine the correlation time (τ_c) for the dipolar effects on ^1H and ^{31}P relaxation. This has been done for the case at hand in two ways. (a) From the frequency dependence of water proton relaxation in the presence of the enzyme–Mn^{2+} complex (both in the presence and in the absence of ATP analogues), dipolar correlation times of (4.5 ± 0.8) × 10^{-9} s at 49.0 MHz have been measured (Table I). In these studies it was determined that τ_c is dominated by τ_s. If this is the case for water proton relaxation of the binary and ternary complexes, it must also be the case that τ_s is the dominant term in the determination of τ_c for the ^{31}P–Mn^{2+} interaction of interest here. (b) The paramagnetic effect of Mn^{2+} on the longitudinal relaxation rates of ^{31}P of the DTT-activated enzyme–Mn^{2+}–$Co(NH_3)_4AMPPCP$ complex was measured at two frequencies: 121.7 and 145.1 MHz. A frequency dependence of the ^{31}P NMR relaxation rate was observed for all nuclei. This verifies the above assumption that τ_s is the dominant term in the determination of τ_c. With the method described by Stewart (1988), these results gave a value of τ_c = 1.0 × 10^{-9} s at 121.7 MHz. Comparison of the τ_c values obtained by the two measurements shows reasonable agreement. The difference that exists may simply reflect the frequency dependence of τ_c itself. Subsequent distance calculations in this work were based on the value of 1.0 × 10^{-9} s determined in the ^{31}P relaxation measurements.

In order that these paramagnetic probe experiments might be used to determine internuclear distances at the active site, the assumption of fast exchange must be quantitatively justified. Temperature measurements were used to provide limits on the exchange rate (Mildvan & Cohn, 1970). In this experiment, a decrease in the relaxation rate with increasing temperature can only correspond to the fast-exchanging region of T_1. Figure 7 shows plots of $1/fT_{1p}$ versus reciprocal temperature for all seven proton nuclei of $Co(NH_3)_4AMPPCP$. The slope of each line is positive, indicating that the fast-exchange condition ($T_{1M} \gg \tau_m$) is satisfied.

Distances from the two divalent cation sites to the phosphorus and hydrogen nuclei of enzyme-bound $Co(NH_3)_4AMPPCP$ were calculated by use of eqs 9 and 10, respectively, and the relaxation data of Figures 5 and 7. As shown in Tables III and IV, the Mn–P and Mn–H distances calculated from site 1, the tight site, are substantially longer than those calculated from site 2, the weaker binding site. For both sites, the Mn–P distances to the β-P and γ-P atoms of the bound substrate are smaller than those to the α-P of $Co(NH_3)_4AMPPCP$. The distances to Mn^{2+} at site 2 are consistent with a distorted inner-sphere complex with the β-P and γ-P of the substrate analogue. All of the other distances are more consistent with second-sphere coordination, which may involve bridging ligands such as solvent molecules or amino acid residues.

Discussion

Proton relaxation measurements of the CF_1 ATPase in the presence of Mn^{2+} and substrates or substrate analogues provide evidence for the formation of stable binary and ternary complexes. From the results of the frequency study (Figure 3), it is apparent that τ_c does not exhibit large changes in the binary versus the ternary latent or activated complex. Therefore, the increased enhancement observed in Figures 1 and 2 must be due either to increased Mn^{2+} bound to CF_1 upon the addition of substrate or to an increase in the water ex-

change rate. Given the observed cooperativity of metal binding to the enzyme (Haddy et al., 1985), the first proposal seems likely.

The K_5 values determined in Table II are less than K_1, consistent with a tightening of metal binding in the presence of substrate. Thus, under the conditions of our experiments, the divalent cation sites are partially occupied by Mn^{2+} in the absence of substrate, but the occupancy of these Mn^{2+} sites is increased upon the addition of substrate. This explains the increase in observed enhancement in Figures 1 and 2 for the substrates P_i, ADP, ATP, $Co(NH_3)_4ADP$, $Co(NH_3)_4ATP$, and $Co(NH_3)_4AMPPCP$. In the case of vanadate, the low enhancement of the E–Mn–VO_4 complex dominates, and the increased binding of metal is apparent from the values of Table II but not from a visual inspection of the plot (Figure 2). Additionally, a comparison of K_2 and K_4 values shows that K_4 is considerably less than K_2 for all ternary complexes. Therefore, the presence of Mn^{2+} lowers the dissociation constant for nucleotides ($K_4 < K_2$), and also, the presence of nucleotides lowers the K_D for Mn^{2+} ($K_5 < K_1$).

Substrate binding constants for ADP, ATP, and vanadate are similar for the latent and activated complexes. Best-fit K_1 and K_5 values (Table II) show good agreement with the literature (Hochman & Carmeli, 1981; Hiller & Carmeli, 1985). There is also good agreement between the fitted K_4 values and literature values for the substrates ADP and ATP (Cantley & Hammes, 1975; Bruist & Hammes, 1981; Frash & Sharp, 1985). As in a number of other ATPases (Grisham, 1988), the Co(III) nucleotides bind much more weakly to the activated EM complex than the "natural" substrates.

The kinetic studies show that $Co(NH_3)_4AMPPCP$ competitively inhibits the calcium-dependent activity of the DTT-activated CF_1 ATPase. The K_i determined in this study agrees with kinetic studies using CrATP (Frasch & Sharp, 1982) but exhibits much weaker inhibition than previously reported inhibition constants for Co(III) nucleotides on CF_1 ATPase (Hochman et al., 1979). The observation of competitive inhibition with CoAMPPCP justifies our subsequent use of this complex as a structural probe of the nucleotide site of CF_1.

The data of Table I and Figures 5 and 7 provide compelling evidence that a ternary Mn^{2+}–$Co(NH_3)_4AMPPCP$-activated enzyme complex is formed under the conditions of these NMR experiments. Previous kinetic (Bruist & Hammes, 1981) and EXAFS studies (Carmeli et al., 1986) are consistent with the premise that Mn^{2+} and $Co(NH_3)_4AMPPCP$ bind to relevant catalytic sites in this complex. However, it is important to point out that the water proton relaxation experiments involved titrations of 1:1 complexes of Mn^{2+} and enzyme—conditions in which only the tight Mn^{2+} sites (Hochman & Carmeli, 1981) are filled. The high-resolution ^{31}P and ^1H NMR experiments, on the other hand, were carried out over a wider range of Mn^{2+} concentrations, so that both Mn^{2+} sites are eventually populated. This is seen most clearly in a comparison of Figures 5 and 7 and Tables III and IV. The paramagnetic effects of low levels of Mn^{2+} on both the phosphorus and hydrogen nuclei of the bound substrate are consistent with effects from the high-affinity Mn^{2+} sites. The dramatic change in paramagnetic effect of Mn^{2+} on the protons of the bound substrate at Mn^{2+} levels exceeding the enzyme concentration, on the other hand, is consistent with Mn^{2+}–substrate interactions on the enzyme from a weaker class of Mn^{2+} sites.

Consideration of exchange rates should permit an assignment of the nucleotide site detected in these studies to one of the nucleotide sites previously observed on CF_1 by others. Since the nucleotide site detected by our NMR studies is shown here to exchange $Co(NH_3)_4AMPPCP$ rapidly with respect to the normalized relaxation rates of Tables III and IV (see Figure 8), the largest of these rates (5.4×10^4 s^{-1}) sets a lower limit for the exchange rate of the nucleotide site detected in these studies. As pointed out earlier, previous studies of nucleotide binding to CF_1 have consistently demonstrated the existence of three nucleotide binding sites per $\alpha_3\beta_3\gamma\delta\epsilon$ enzyme multimer, designated sites 1, 2, and 3 (Bruist & Hammes, 1981, 1982; Cantley & Hammes, 1975). Site 1 is believed to be a regulatory binding site for ADP. Exchange of ADP from this site is slow, with an exchange half-time of at least 30 min, except during the catalytic cycle when the exchanging rate apparently increases. Thus, it is unlikely that this site is the site observed in our NMR studies. Site 2 binds MgATP preferentially with a K_D of 1 μM. Here also the nucleotide is tightly bound and not easily removed by dialysis, gel filtration, or catalytic turnover. Exchange half-times for nucleotide at this site are on the order of days (Bruist & Hammes, 1981). This site is thus unlikely to be the nucleotide site observed in the present NMR studies. On the other hand, nucleotide bound at site 3 has been shown to exchange rapidly, and this site is presumed to be the catalytic site for CF_1. Given the rapid exchange of nucleotide at this site, and the good agreement between the kinetic constants and the dissociation constants determined from the water proton relaxation studies (Table II and references cited therein), it is reasonable to suggest that the nucleotide site characterized in the present NMR studies is the catalytic nucleotide site of CF_1.

The calculations of site to site distances involving metal and ATP sites are complicated by the fact that Mn^{2+} is known to bind to two or three tight sites and three weaker sites on the enzyme (Hiller & Carmeli, 1985; Haddy et al., 1985). No information is available to suggest the exact location of these metal sites. The β subunit has been implicated in nucleotide binding (Bruist & Hammes, 1981), and on the basis of the accepted stoichiometry, the enzyme contains three symmetrically arranged β subunits (Boekema et al., 1988). The simplest possible model would link the three tight and three weak metal sites, both structurally and functionally, with the three nucleotide sites. Although the phosphorus and proton relaxation data of Tables III and IV do not involve the slow-exchanging nucleotide sites 1 and 2, our data are consistent with a model that contains one tight and one weak Mn^{2+} binding site at the catalytic nucleotide binding site (site 3). Support for this notion is provided by Haddy et al. (1989), who show that the catalytic nucleotide site binds metal–nucleotide complexes preferentially over free nucleotide. Moreover, the best fit to our nuclear relaxation data requires the existence on the enzyme of two different classes of Mn^{2+} binding sites (Hochman & Carmeli, 1981a; Haddy & Sharp, 1989) and employs the same binding constants previously determined for the binding of Mn^{2+} to high-affinity and low-affinity metal sites on the enzyme (Hochman & Carmeli, 1981a). The good agreement between these binding constants and the constants K_1 and K_5 obtained in the water proton relaxation experiments (Table II) make it likely that the tight site observed in our high-resolution NMR studies, the site observed by water proton relaxation, and the tight site described by Hochman and Carmeli are one and the same. Additional evidence of consistency between the present work and previous studies of metal and substrate binding to CF_1 can be found in the analysis of the frequency dependence of water relaxation in the presence of substrates (Table I). Our values for q, the number of fast-exchanging water molecules,

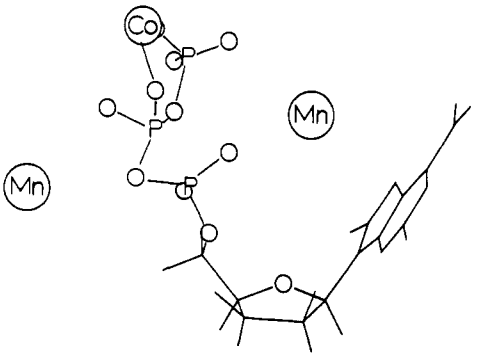

FIGURE 9: Conformation of the $Co(NH_3)_4AMPPCP$ and the enzyme-bound Mn^{2+} ions at the active site of CF_1 ATPase from spinach. The structure was derived on a Silicon Graphics workstation using MMS software with the distances determined from the magnetic resonance experiments. Calculated distances are based on a dipolar correlation time of 1.0×10^{-9} s.

at the tight Mn^{2+} site in the presence of ATP and ADP of 1.7 and 2.3, respectively, compare quite well with those of Haddy et al. (1989), who obtained values of 1.8 and 2.9, respectively.

The distances in Tables III and IV show that the weak metal binding site is closest to the substrate analogue within the active site. This finding contradicts the suggestion that the tight sites are the *only* sites near the catalytic site as was earlier postulated (Carmeli et al., 1986). The distances are too large to be purely inner-sphere complexes (Grisham & Mildvan, 1974). The Mn^{2+}–P distances for site 1 (the tight site) are consistent with second-sphere coordination values. The Mn^{2+}–P distances for site 2 (the weak site) are consistent with coordination of the metal to the β- and γ-phosphates of the triphosphate chain and the formation of a "distorted" inner-sphere complex between the Mn^{2+} and the β- and γ-phosphates. The only direct physical evidence from the literature for the involvement of a divalent metal–ATP complex and its conformation comes from EXAFS studies on the latent enzyme where the average Mn^{2+}–O and Mn^{2+}–P bond distances were found to change significantly in the Mn^{2+}–ATP–enzyme complex versus the hydrated Mn^{2+} ion and Mn^{2+}–ATP (Carmeli et al., 1986). An average Mn^{2+}–P distance of 4.95 ± 0.15 Å was obtained in the EXAFS study. The average Mn^{2+}–P value obtained from our data is 5.29 ± 0.5 Å. Differences between the two values may reflect changes in conformation from latent to activated enzyme or merely differences in the two measurements.

Our data show that the Mn^{2+} sites are in fact close to the nucleotide site. In such a case, the data of Tables III and IV should provide information on the conformation of the ATP at the active site of the CF_1 ATPase. The data of Tables III and IV are consistent with a model for the active site in which the nucleotide adopts a bent or folded conformation and the "site 1" Mn^{2+} is directly in front of the phosphate chain while the "site 2" Mn^{2+} is in the cleft above the ribose ring, and between the triphosphate and adenine moieties of the bound substrate. This model, developed with the distances calculated in the present study, is shown in Figure 9. The conformation of the $Co(NH_3)_4AMPPCP$ has the glycosidic bond linking the adenine base to the ribose sugar in the syn conformation. The torsional angle about the $C_{1'}$–N_9 bond that links the base to the sugar is denoted by χ. The sequence of atoms defining this angle is $O_{4'}$–$C_{1'}$–N_9–C_8. The term anti refers to χ values of 0° ± 90°, while syn refers to values of 180° ± 90°. The value of χ determined from the model built from the data of Tables III and IV is 112°. The anti conformation is generally found in purine nucleotides and complexes in both crystalline and solution structures (Saenger, 1984). However, the glycosidic torsional angle (χ) for AMP bound to adenylate kinase was found to be 110° (Fry, 1988, 1985). As shown in Figure 10, the conformation of the ribose ring is slightly N-type (in which $C_{2'}$ is endo and $C_{3'}$ is exo) (Altona & Sundaralingam, 1973). The torsional angle δ is indicative of the puckering in the ribose and is defined by the atom sequence $C_{5'}$–$C_{4'}$–$C_{3'}$–$O_{3'}$ (Saenger, 1984). The δ value measured for CF_1 ATPase bound $Co(NH_3)_4AMPPCP$ is 126°. The orientation of $O_{5'}$ relative to the ribose ring is determined by the torsional angle γ, defined by the sequence $O_{5'}$–$C_{5'}$–$C_{4'}$–$C_{3'}$ (Saenger, 1984). The value of γ measured in the present model is 162°. The conformation of ATPase-bound $Co(NH_3)_4AMPPCP$ in terms of χ, δ, and γ is shown in Figure 10.

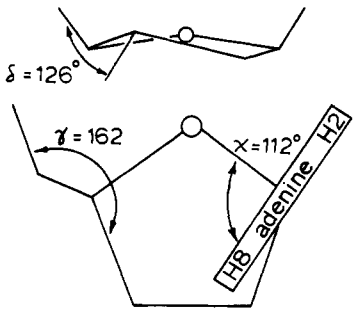

FIGURE 10: Two views of the ribose ring of $Co(NH_3)_4AMPPCP$ bound to the CF_1 ATPase. The structure is derived from the distances calculated from the paramagnetic relaxation measurements in Tables III and IV. The torsional angles χ, δ, and γ are shown for the bound $Co(NH_3)_4AMPPCP$.

Table V: Protein-Bound Nucleotide Conformations of Representative Enzymes

enzyme	substrate	τ (deg)	δ (deg)	χ (deg)
CF_1 ATPase	CoAMPPCP	162	126	112
Na,K-ATPase[a]	$Co(NH_3)_4ATP$	178	100	35
Ca^{2+}-ATPase[b]	CoAMPPCP	160	120	110
adenylate kinase[c]	AMP	180	105	110
adenylate kinase fragment[c]	MgATP	50	94	65
protein kinase[d]	$Co(NH_3)_4ATP$			78

[a] Stewart and Grisham (1988); Stewart et al. (1989). [b] Kuntzweiler (1988); Kuntzweiler and Grisham (1989). [c] Fry et al. (1985, 1987). [d] Rosevear et al. (1983).

It should be noted that absolute Mn^{2+}–phosphorus and Mn^{2+}–proton distances depend on accurate knowledge of the dipolar correlation time (see eqs 9–11). The dipolar correlation time determined from the frequency dependence of the ^{31}P NMR relaxation rate (1.0×10^{-9} s) was used in the distance calculations of Tables III and IV.

The proposed nucleotide conformation at the active site of CF_1 ATPase is compared to previously determined nucleotide conformations in a variety of other enzymes in Table V. The γ and δ values vary to some degree between the three ATPases studied, but the difference in χ is most notable. The χ value for the CF_1 ATPase is more similar to the value obtained for AMP in adenylate kinase (Fry et al., 1985, 1987). It is particularly interesting to note similarities and differences among the ATPases studied. Na, K-ATPase is a "P-type" ATPase (Pedersen, 1987). Compared to CF_1, it is a relatively smaller (110–150 kDa) and structurally simple integral membrane protein. This class of enzymes can exist in two different conformational states (E_1 and E_2), and the reaction pathway of this class of enzymes is characterized by a phosphorylated enzyme intermediate. The CF_1 ATPase is an "F-type" ATPase (Pedersen, 1987). As such, it is structurally larger and more complex than the Na,K-ATPase. The ATPase portion of the CF_1 ATPase is a soluble protein. The

reaction mechanism of this class of ATPases does not appear to proceed through a phosphorylated enzyme intermediate, but rather the F-type ATPases catalyze a reaction cycle that involves the tight binding of ATP. The electrochemical proton gradient is proposed to induce a conformational change in the enzyme that leads to ATP release. These differences among the ATPases studied may account for the variation in their active site structure.

The results described here are fully consistent with the model of the metal and nucleotide sites of CF_1 proposed by Haddy et al. (1989). In this model, two metal ions can bind at or near nucleotide sites 2 and 3 with high affinity in the absence of added nucleotide. Binding of nucleotide to these sites enhances the binding of metal and alters the structural and magnetic properties of the metals. Our data support this model but also indicate that the high-affinity metal at the catalytic site is near, but not directly coordinated to, the bound nucleotide substrate. As shown in Figure 9, this high-affinity metal is near enough to the triphosphate moiety of the substrate to form a second-sphere complex with the β-P and γ-P of the bound substrate. Such coordination could explain the structural and magnetic effects observed by Haddy et al., without requiring direct coordination of the high-affinity metal by the bound nucleotide.

ACKNOWLEDGMENTS

We acknowledge Dr. Mark T. Devlin for writing and providing RCALC, the program used to fit the ^{31}P and ^{1}H relaxation data.

REFERENCES

Altona, A., & Sundaralingam, M. (1973) *J. Am. Chem. Soc. 95*, 2333.
Armstrong, R. N., Kondo, H., Granot, J., Kaiser, E. T., & Mildvan, A. S. (1979) *Biochemistry 18*, 1230–1238.
Benkovic, S. J., Engle, J., & Mildvan, A. S. (1972) *Biochem. Biophys. Res. Commun. 47*, 852–858.
Bernheim, R., Brown, T., Gutkowsky, H., & Woessner, D. (1959) *J. Chem. Phys. 30*, 950.
Binder, A., Jagendorf, A., & Ngo, E. (1978) *J. Biol. Chem. 253*, 3094–3100.
Bloembergen, N. (1957) *J. Chem. Phys. 27*, 572–579.
Boekema, E. J., van Heel, M., & Graber, P. (1988) *Biochim. Biophys. Acta 933*, 365–371.
Bruist, M. F., & Hammes, G. G. (1981) *Biochemistry 20*, 6298–6305.
Bruist, M. F., & Hammes, G. G. (1982) *Biochemistry 21*, 3370–3377.
Cantley, L. C., & Hammes, G. G. (1975) *Biochemistry 14*, 2968–2975.
Cantley, L. C., & Hammes, G. G. (1976) *Biochemistry 15*, 9–14.
Carlier, M. F., & Hammes, G. G. (1979) *Biochemistry 18*, 3446–3451.
Carmeli, C., Huang, J. Y., Mills, D. M., Jagendorf, A. T., & Lewis, A. (1986) *J. Biol. Chem. 261*, 16969–16975.
Cerione, R. A., McCarty, R. E., & Hammes, G. G. (1983) *Biochemistry 22*, 769–776.
Cornelius, R. D., Hart, P. A., & Cleland, W. W. (1977) *Inorg. Chem. 16*, 2799–2805.
Craik, D. J., & Levy, G. C. (1984) in *Topics in ^{13}C NMR Spectroscopy* (Levy, G. C., Ed.) Vol. 4, pp 239–275, Wiley, New York.
Devlin, C. (1989) Ph.D. Dissertation, University of Virginia.
Devlin, C., & Grisham, C. M. (1988) *FASEB J. 2*, A1743.
Eisinger, J., Shulman, R. G., & Szymanski, B. M. (1962) *J. Chem. Phys. 36*, 1721–1729.
Frasch, W. D., & Selman, B. R. (1982) *Biochemistry 21*, 3636–3643.
Frasch, W. D., & Sharp, R. R. (1985) *Biochemistry 24*, 5454–5458.
Fry, D. C., Kuby, S. A., & Mildvan, A. S. (1985) *Biochemistry 24*, 4680–4694.
Fry, D. C., Kuby, S. A., & Mildvan, A. S. (1987) *Biochemistry 26*, 1645–1655.
Goodno, C. C. (1982) *Methods Enzymol. 85*, 116–123.
Grisham, C. M. (1988) *Methods Enzymol. 156*, 353–371.
Haddy, A. E., & Sharp, R. R. (1989) *Biochemistry 28*, 3656–3664.
Haddy, A. E., Frasch, W. D., & Sharp, R. R. (1985) *Biochemistry 24*, 7926–7930.
Haddy, A. E., Frasch, W. D., & Sharp, R. R. (1989) *Biochemistry 28*, 3664–3669.
Hiller, R., & Carmeli, C. (1985) *J. Biol. Chem. 260*, 1614–1617.
Hochman, Y., & Carmeli, C. (1981a) *Biochemistry 20*, 6287–6292.
Hochman, Y., & Carmeli, C. (1981b) *Biochemistry 20*, 6293–6297.
Hochman, Y., Lanir, A., & Carmeli, C. (1976) *FEBS Lett. 61*, 255–259.
Hochman, Y., Lanir, A., Werber, M. M., & Carmeli, C. (1979) *Arch. Biochem. Biophys. 192*, 138–147.
Klemens, M. R. (1987) Ph.D. Thesis, University of Virginia.
Kuntzweiler, T. A. (1988) M.S. Thesis, University of Virginia.
Kuntzweiler, T. A., & Grisham, C. M. (1989) *Biochemistry* (submitted for publication).
Laemmli, U. K. (1970) *Nature 227*, 680–685.
Leckband, D., & Hammes, G. G. (1987) *Biochemistry 26*, 2306–2312.
Levy, G. C., & Peat, I. R. (1975) *J. Magn. Reson. 18*, 500–521.
Lowry, O. H., Rosebrough, N. J., Farr, A. L., & Randall, R. J. (1951) *J. Biol. Chem. 193*, 265–275.
Macara, I. G. (1980) *Trends Biol. Sci. 5*, 92–94.
McClaugherty, S. H., & Grisham, C. M. (1982) *Inorg. Chem. 21*, 4133–4138.
Merritt, E. A., Sundaralingam, M., Cornelius, R. D., & Cleland, W. W. (1978) *Biochemistry 17*, 3274.
Mildvan, A. S., & Cohn, M. (1966) *J. Biol. Chem. 241*, 1178–1193.
Mildvan, A. S., & Cohn, M. (1970) *Adv. Enzymol. Relat. Areas Mol. Biol. 33*, 1–70.
Mildvan, A. S., & Engle, J. (1972) *Methods Enzymol. 26C*, 654–682.
Mildvan, A. S., & Grisham, C. M. (1974) *Struct. Bonding (Berlin) 20*, 1–21.
Musier, K. M., & Hammes, G. G. (1987) *Biochemistry 26*, 5982–5988.
Pedersen, P. L., & Carafoli, E. (1987) *Trends Biol. Sci. 12*, 146–150.
Penefsky, H. S. (1977) *J. Biol. Chem. 252*, 2891–2899.
Reed, G. H., Cohn, M., & O'Sullivan, W. J. (1970) *J. Biol. Chem. 245*, 6547.
Reuben, J., & Cohn, M. (1970) *J. Biol. Chem. 245*, 6539.
Rosevear, P. R., Bramson, H. N., O'Brian, C., Kaiser, E. T., & Mildvan, A. S. (1983) *Biochemistry 22*, 3439–3447.
Saenger, W. (1984) *Principles of Nucleic Acid Structure* Springer-Verlag, New York.
Solomon, I. (1955) *Phys. Rev. 99*, 559.

Solomon, I., & Bloembergen, N. (1956) *J. Chem. Phys. 25*, 261.
Stewart, J. M. M., & Grisham, C. M. (1988) *Biochemistry 27*, 4840–4848.
Stewart, J. M. M., Jørgensen, P. L., & Grisham, C. M. (1989) *Biochemistry 28*, 4695–4701.
Viswamitra, M. A., Hosur, M. V., Shakked, Z., & Kennard, O. (1976) *Cryst. Struct. Commun. 5*, 819.

EPR Characterization of Genetically Modified Reaction Centers of *Rhodobacter capsulatus*†

Edward J. Bylina,‡,§ Stephen V. Kolaczkowski,‖,⊥ James R. Norris,‖ and Douglas C. Youvan*,‡
Department of Chemistry, Massachusetts Institute of Technology, Cambridge, Massachusetts 02139, and Chemistry Division, Argonne National Laboratory, Argonne, Illinois 60439
Received October 3, 1989; Revised Manuscript Received March 9, 1990

ABSTRACT: Electron paramagnetic resonance (EPR) has been used to investigate the cation and triplet states of *Rhodobacter capsulatus* reaction centers (RCs) containing amino acid substitutions affecting the primary donor, monomeric bacteriochlorophylls (Bchls), and the photoactive bacteriopheophytin (Bphe). The broadened line width of the cation radical in $His^{M200} \rightarrow Leu$ and $His^{M200} \rightarrow Phe$ reaction centers, whose primary donor consists of a Bchl–Bphe heterodimer, indicates a highly asymmetric distribution of the unpaired electron over the heterodimer. A T_0 polarized triplet state with reduced yield is observed in heterodimer-containing RCs. The zero field splitting parameters indicate that this triplet essentially resides on the Bchl half of the heterodimer. The cation and triplet states of reaction centers containing $His^{M200} \rightarrow Gln$, $His^{L173} \rightarrow Gln$, $Glu^{L104} \rightarrow Gln$, or $Glu^{L104} \rightarrow Leu$ substitutions are similar to those observed in wild type. Oligonucleotide-mediated mutagenesis has been used to change the histidine residues that are positioned near the central Mg^{2+} ions of the reaction center monomeric bacteriochlorophylls. Reaction centers containing serine substitutions at M180 and L153 or a threonine substitution at L153 have unaltered pigment compositions and are photochemically active. The cation and triplet states of $His^{L153} \rightarrow Leu$ reaction centers are similar to those observed in wild type. Triplet energy transfer to carotenoid is not observed at 100 K in $His^{M180} \rightarrow Arg$ chromatophores. These results have important implications for the structural requirements of tetrapyrrole binding and for our understanding of the mechanisms of primary electron transfer in the reaction center.

The photosynthetic reaction center (RC) mediates extremely efficient electron-transfer reactions that result in high quantum yields for the conversion of light to chemical energy (Kirmaier & Holten, 1987; Okamura et al., 1982). Crystal structures have been determined for RCs from both *Rhodopseudomonas viridis* (Deisenhofer et al., 1984, 1985) and *Rhodobacter sphaeroides* (Chang et al., 1986; Allen et al., 1986). Although the crystal structure of RCs from *Rhodobacter capsulatus* has not been determined, extensive sequence similarities among these three species [see review in Komiya et al. (1988)] facilitate mutagenesis experiments in *Rb. capsulatus*. Genetic tools are most advanced for this species (Scolnik & Marrs, 1987). RC and light-harvesting genes have been deleted from the *Rb. capsulatus* chromosome (Youvan et al., 1985). Such deletions may be complemented by plasmids (Bylina et al., 1986, 1989) bearing either wild-type or mutagenized copies of the RC genes. Recently, mutations affecting the properties of the primary donor in RCs of *Rb. capsulatus* have been generated and characterized. The primary donor in $His^{M200} \rightarrow Leu$ and $His^{M200} \rightarrow Phe$ reaction centers consists of a heterodimer of bacteriochlorophyll (Bchl) and bacteriopheophytin (Bphe) (Bylina & Youvan, 1988). Time-resolved optical measurements indicate that the quantum yield of the initial electron-transfer reaction in $His^{M200} \rightarrow Leu$ reaction centers is reduced by about half (Kirmaier et al., 1988). Substitutions at glutamic acid residue L104, which interacts with the photoactive Bphe, indicate that glutamic acid-L104 is largely responsible for the spectroscopic red shift of this pigment but that the interaction is not the dominant contributor to the directionality of electron transfer in reaction centers (Bylina et al., 1988b).

Histidines-L153 and -M180 of the *Rps. viridis* reaction center act as axial ligands to the central Mg^{2+} ions of the monomeric Bchl molecules, which are in van der Waals contact with both the primary donor (special pair Bchls) and the RC Bphes (Michel et al., 1986). Refined crystallographic data (Yeates et al., 1988) from *Rb. sphaeroides* suggest that while the M-subunit histidines act as axial ligands to their associated Bchls, the L-subunit histidines (L153 and L173) associated with RC Bchls do not directly ligand the Bchl Mg. One of these monomeric Bchls can be removed from *Rb. sphaeroides* reaction centers by treatment with $NaBH_4$, resulting in the reduction of the ground-state absorption band at 800 nm while leaving the remainder of the absorption spectrum unaffected (Ditson et al., 1984). Reaction center photochemistry is

† This work was supported by the National Science Foundation (DMB-8609614) and the U.S. Department of Agriculture (87-CRCR-1-2328). Work at ANL was supported by the U.S. Department of Energy, Office of Basic Energy Sciences, Division of Chemical Sciences, under Contract W-31-109-Eng-38.
* Address correspondence to this author.
‡ Massachusetts Institute of Technology.
§ Present address: Biotechnology Program, Pacific Biomedical Research Center, University of Hawaii at Manoa, Honolulu, HI 96822.
‖ Argonne National Laboratory.
⊥ Present address: Department of Chemistry, University of Arizona, Tucson, AZ 85721.

0006-2960/90/0429-6203$02.50/0